Surface Science 606 (2012) 1426–1430

Contents lists available at SciVerse ScienceDirect

Surface Science

journal homepage: www.elsevier.com/locate/susc

Surface contributions to the XPS spectra of nanostructured NiO deposited on HOPG

I. Preda [a], R.J.O. Mossanek [b], M. Abbate [b], L. Alvarez [c], J. Méndez [c], A. Gutiérrez [a], L. Soriano [a,*]

[a] Departamento de Física Aplicada and Instituto de Ciencia de Materiales Nicolás Cabrera, Universidad Autónoma de Madrid, Cantoblanco, 28049 Madrid, Spain
[b] Departamento de Física, Universidade Federal do Paraná, Caixa Postal 19044, 81531-990 Curitiba PR, Brazil
[c] Instituto de Ciencia de Materiales de Madrid, ICMM-CSIC, Cantoblanco, 28049 Madrid, Spain

ARTICLE INFO

Article history:
Received 27 September 2011
Accepted 7 May 2012
Available online 14 May 2012

Keywords:
Photoemission in NiO
Surface effects
NiO nanostructures

ABSTRACT

In this work we present an *in situ* X-ray photoelectron spectroscopy (XPS) study of the growth of NiO on highly ordered pyrolitic graphite (HOPG). The XPS spectra were measured as a function of the equivalent NiO coverage. Also, *ex-situ* atomic force microscopy (AFM) images were taken for some of these stages in order to follow the morphology of the NiO deposits. For low coverages the lineshapes of the Ni 2p spectra differ strongly from those of bulk NiO. This has been related to the large surface contribution. The O 1s XPS spectra also show a surface related structure which follows the same trend observed in the Ni 2p spectra.

1. Introduction

In previous works, we concluded that both, surface and non-local effects are present in the Ni 2p XPS spectra. This was deduced by means of configuration interaction cluster calculations [1,2]. These calculations were compared to the Ni 2p XPS experimental spectra of a NiO bulk sample taken in different experimental conditions (incident angle, photon energy) in order to vary the surface sensitivity of the spectra. In the present work we present experimental data which are also explained by our surface and non-local model, however, in this case, the experimental conditions of the spectra are the same whereas the surface-to-bulk ratio changes with the morphology of the NiO nanostructures, where this ratio is considerably enhanced. It is shown below that this model is completely consistent in the explanation of the Ni 2p XPS spectra of the observed NiO nanostructures. Atomic force microscopy (AFM) images obtained for both, the early and final stages of growth, support the conclusions obtained in this work. Finally, we show that the O 1s XPS spectra present similar trends and the interpretation is in agreement with the Ni 2p spectra.

NiO is a charge transfer oxide in which the ground state is a mixture of $3d^8$, $3d^9\underline{L}$, and $3d^{10}\underline{L}^2$ configurations, where $\underline{L}$ denotes a hole at the ligand (oxygen) site. This electronic structure gives rise to a Ni 2p spectrum with multiple peaks, which have been widely discussed in the literature [3–5]. Nowadays, it is accepted that the broad satellite located at about 863 eV binding energy corresponds to $\underline{c}3d^{10}\underline{L}^2$ and $\underline{c}3d^8$ transitions, whereas the main peak located at 854.5 eV binding energy is assigned to $\underline{c}3d^9\underline{L}$ transitions, where $\underline{c}$ denotes a Ni 2p core level hole (see Fig. 1). However, the origin of the shoulder, shifted by 1.5 eV towards higher binding energy with respect to the main peak, has been a matter of discussion for years. It was initially assigned to Ni^{3+} ions [6,7], although it is currently interpreted as a non-local screening satellite [8]. The intensity of this shoulder is also very sensitive to the presence of defects [9]. Photoemission studies on NiO observed that its intensity was affected by the take off angle of the measurements [10,11]. Later on, this has been attributed to surface effects due to the Ni atoms in pyramidal coordination at the NiO surface [1]. More recently, Taguchi et al. [12] explained the Ni 2p spectra of NiO in terms of Zhang-Rice (ZR) doublet bound states. In a recent paper, we describe both non-local and surface effects within a single configuration interaction model [1,2].

According to our model [2], the shoulder has two contributions (see Fig. 1): one coming from nonlocal screening, in agreement with van Veenendaal et al. [6]; and another due to the Ni ions in pyramidal symmetry at the surface. In this way, the model is able to explain the Ni 2p photoemission spectra for any photon energy and/or take-off angle. We have shown that the experimental Ni 2p spectra can be fitted with four curves to describe the main line, the shoulder and the satellite. The main line ($\underline{c}3d^9\underline{L}$) comes from octahedrally coordinated NiO_6 clusters (bulk); the shoulder comes from nonlocal charge fluctuations and pyramidally coordinated NiO_5 clusters (surface); and finally, the satellite comes from other contributions [2].

Previous studies on the growth of NiO deposited on highly oriented pyrolitic graphite (HOPG) were published elsewhere [13,14]. In these works, the O 1s X-ray absorption spectra (XAS) of very early stages of growth show that the unoccupied Ni e_g states are split for the Ni ions located at the surface. This result is also in agreement with the O 1s XAS spectra of 3–5 nm NiO nanoparticles [15]. The morphology of the early and final states of the growth of NiO has also

* Corresponding author. Fax: +34 914973969.
E-mail address: l.soriano@uam.es (L. Soriano).

0039-6028/$ – see front matter © 2012 Elsevier B.V. All rights reserved.
doi:10.1016/j.susc.2012.05.005

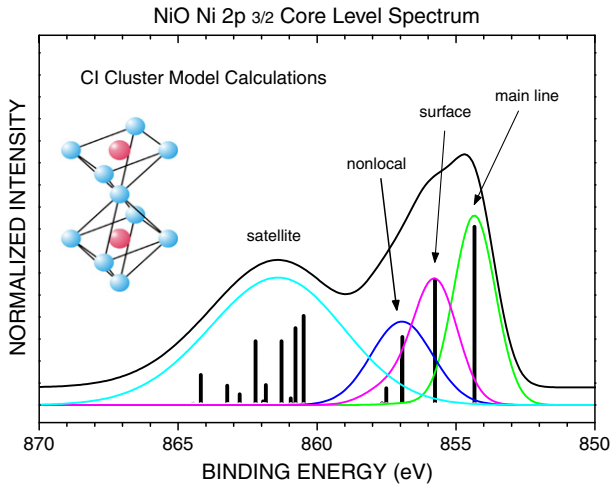

Fig. 1. Cluster model calculations of the Ni 2p XPS spectrum (taken from Ref. [2]). The calculations are performed using an octahedral NiO_6 cluster in contact with a pyramidal NiO_5 cluster.

been studied using atomic force microscopy (AFM) [16]. In this work, the AFM results are compared with those obtained by the analysis of the inelastic background by means of the Quases software [17]. The agreement between both techniques was excellent. Studies on nanostructures of Ni and NiO deposited on different substrates have also been reported in the literature: [18–23]. Biju et al. [18] studied the electronic structure of 4–5 nm NiO nanoparticles by Ni 2p XPS analysis. They concluded that the increase of the intensity of the shoulder was due to an enhancement of the nonlocal effect for such small nanoparticles. On the other hand, metallic Ni deposited on HOPG gives rise to a Volmer Weber way of growth with the formation of Ni clusters [19]. However, oxidation of the Ni clusters produce the oxidation to NiO but a metallic layer at the interface remains unoxidized [20]. Other interesting results show the reduction of the NiO substrate when metallic Fe is evaporated on it [22]. Core-shell NiO/Ni nanoparticles have also been studied [21]. In these nanoparticles, the metallic Ni core remains stable upon further oxidation. Also, the survey XPS spectra of a NiO thin film deposited on a pure Ni substrate has been simulated [23] using the above referred Quases software [17].

2. Experimental details

The experiment consisted of successive *in situ* depositions of NiO on a HOPG substrate by reactive evaporation of Ni. The evaporation was performed in an oxygen atmosphere (5×10^{-5} Torr) at room temperature. The evaporation rate was constant and maintained low enough to allow the study of the early stages of the growth of NiO on the substrate. After the deposition of a large coverage (~140 monolayers), the sample was annealed at 400 °C for 30 min in ultra high vacuum (5×10^{-9} Torr). This sample was used as a reference of bulk NiO. More details on the sample preparation and characterization can be found elsewhere [13].

The samples were grown in a preparation chamber attached to a CLAM4 XPS spectrometer from Thermo Fisher Scientific. The photoemission spectra were collected using a Mg K_α anode and the pass energy was set at 20 eV. The estimated overall energy resolution (X-rays + analyzer) was about 0.9 eV. The energy scale was calibrated by adjusting the main line of the XPS spectra of NiO at 854.5 eV. The AFM images were measured in dynamic (tapping) mode, using a Nanotec microscope and software [24].

3. Results and discussion

3.1. The Ni 2p 3/2 XPS

Fig. 2 shows the Ni 2p 3/2 XPS spectra of NiO deposited on HOPG as a function of the coverage. The coverage for each step of growth was calculated by different methods. Firstly, an equivalent coverage, i.e., the number of equivalent NiO monolayers present in the sample, was estimated from the intensities of the XPS spectra following conventional methods (exponential growth of the Ni 2p intensity) [25]. Then, the real and equivalent coverages were estimated by the inelastic peak shape analysis, using the QUASES software [17]. Finally, the real coverage was deduced from the AFM images by means of a flooding analysis. The results of these methods showed an excellent agreement. Since the AFM data (see below) show that NiO grows on HOPG forming nanometric islands as the early stages of growth (Volmer–Weber way of growth), the coverages given in monolayers (ML) should be understood as an equivalent coverage. The spectrum of the annealed 140 ML NiO film reproduces previous spectra for bulk NiO [8,9] (see also the Ni 2p 3/2 XPS spectra of a NiO (100) single crystal shown in Fig. 4). This indicates that a stoichiometric NiO film can be grown on HOPG, in agreement with previous X-ray absorption spectroscopy (XAS) studies [13,14]. The peak at 854.5 eV corresponds to the main line ($\underline{c}3d^9\underline{L}$), whereas the peak at 856.0 eV corresponds to the shoulder, which according to our model includes the nonlocal and surface contributions. The most important feature observed in Fig. 2 is that the spectra for low coverage (up to ~40 equivalent ML) differ significantly from that of bulk NiO. In these spectra, the main-line and satellite peaks are

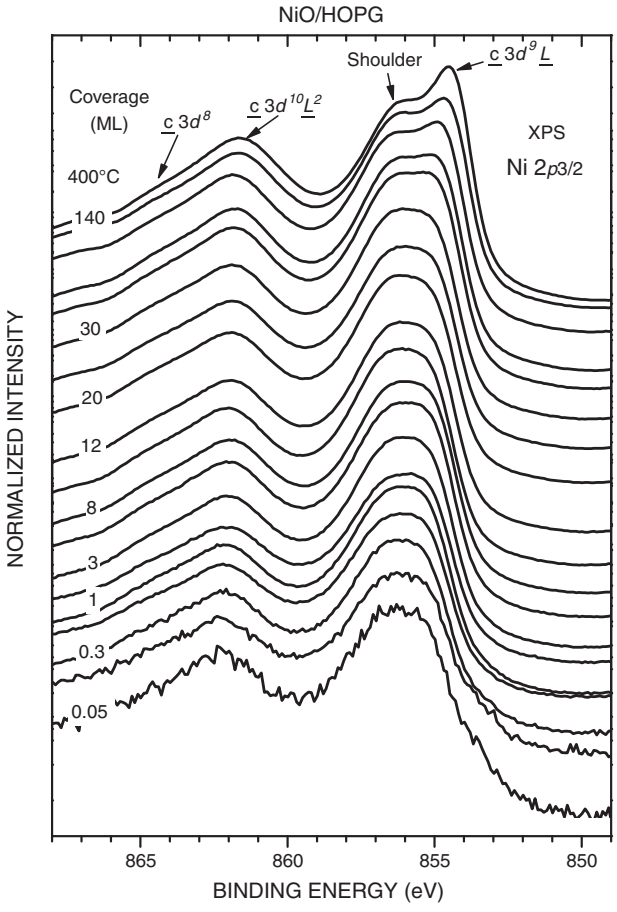

Fig. 2. Ni 2p 3/2 XPS spectra of NiO deposited on HOPG as a function of the equivalent coverage.

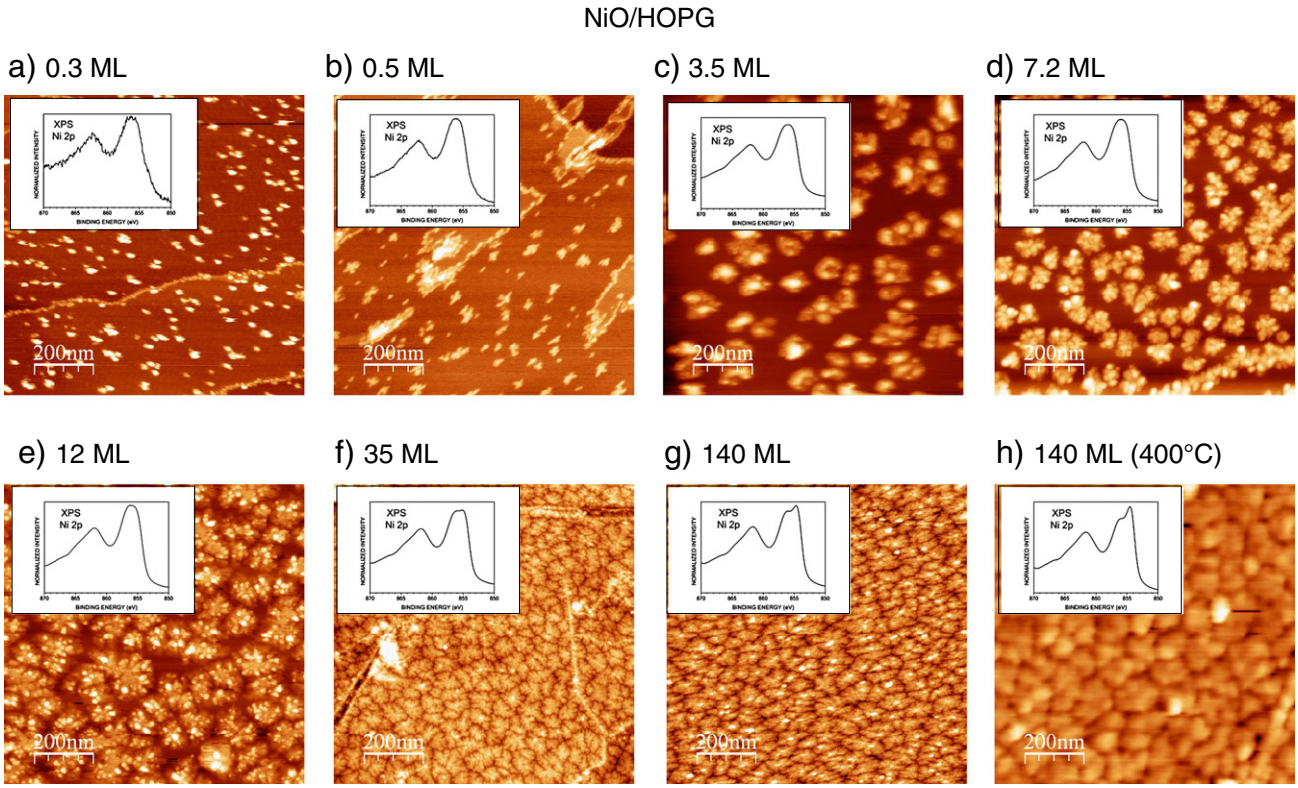

Fig. 3. 200 nm × 200 nm AFM images of NiO deposited on HOPG as a function of the equivalent coverage. The insets show the corresponding Ni 2p 3/2 XPS spectra for each stage of growth.

not completely resolved, giving a broad structure with a width of about 3 eV. We show below that this structure is dominated by the surface contribution.

Fig. 3 shows the AFM images of different stages of growth of NiO on HOPG. For 0.3–0.5 ML equivalent coverage, the nucleation centers consist of 10 nm quasi-spherical NiO nanoparticles which are mostly spread through the terraces. For 3.5–12 ML equivalent coverage, the images show that the previous nucleation centers agglutinate forming aggregates of about 100 nm in size. It is worthy to note here that although the new aggregates are formed by the accumulation of the previous nucleation centers, the effective surface area of the aggregates is slightly lower than the addition of the surfaces of the nucleation centers. This effective surface is slightly decreasing as the number of nucleation centers increases to form the aggregates. For 35–40 ML equivalent coverage, the coalescence of these aggregates is observed. Finally, for the 140 ML equivalent coverage, the aggregates form a continuous film. When this film is submitted to thermal annealing at 400 °C the grain size remains the same as before, but the nanostructures within the grains disappear. As deduced from the images shown in Fig. 3, the way of growth of NiO on HOPG can be regarded as a Volmer–Webber way of growth, i.e., the formation of nanometric islands until coalescence is produced for an equivalent coverage of about 40 ML.

The insets of the AFM images show the corresponding Ni 2p 3/2 XPS spectra for each stage of growth. For the early stages, where the deposits consist mainly of NiO nanoparticles (dispersed and aggregated nucleation centers), the Ni 2p 3/2 XPS spectra show mostly a broad structure. Only when coalescence has been produced, the spectra start to resemble that of bulk NiO. This is obtained only when the NiO thin film has been submitted to thermal annealing, thus producing the aggregation of the nanospheres.

Fig. 4 shows the fittings of the Ni 2p XPS spectra using the three curves (bulk, surface and nonlocal) described above. Also the spectrum of a NiO (100) single crystal measured with the same experimental conditions as the others has been included for comparison. The volume-to-surface ratio given by I_M/I_S, where I_M and I_S stand for the intensities of the main line and surface peak respectively, is also given for each spectrum. The small differences in the fittings and consequently in the I_M/I_S (1.80 vs. 1.84) can be explained as a slight increase of the effective surface of the thin film due to a larger roughness with respect to the single crystal. The curves representing the charge transfer satellite, located around 862 eV, have been omitted in the fittings for clarity reasons. A Shirley background has been subtracted from the spectra prior to the fittings. The energy position, width and relative intensity of the main line (green) and nonlocal (blue) peaks were kept constant throughout the series. The position and width of the surface peak (magenta) were kept constant whereas the intensity was kept free throughout all the fittings. First, we note an excellent agreement with the experimental spectra presented in Fig. 2. For the early stages of growth, the intensity of the surface peak is much larger than that of the main-line (bulk) peak. The surface contribution slightly decreases throughout the intermediate stages of growth due to the loss of effective surface upon aggregation. Only when coalescence is being produced, this ratio increases rapidly up to the value of a bulk thin film ($I_M/I_S = 1.8$).

According to the above results, our model is able to explain and reproduce the experimental Ni 2p XPS spectra of the NiO nanostructured formed on the HOPG substrate. In fact, it is able to interpret the different NiO spectra where the volume-to-surface ratio is varied by varying the experimental conditions, either by varying the inelastic mean free path of the photoelectrons or the photon energy, but also those taken with the same experimental conditions where the volume-to-surface ratio varies according to the morphology of the NiO nanostructures. Besides, our model is consistent not only with the spectrum of a NiO monolayer grown on MgO, the spectrum of a Ni impurity diluted in MgO ($Ni_{0.1}Mg_{0.9}O$) and the calculations of a Ni_6O_{30} cluster [2] but also with some results appeared recently in the literature for NiO nanostructures. For instance, the shape of the Ni 2p XPS spectrum assigned to NiO in the NiO/Ni core shell nanoparticles obtained

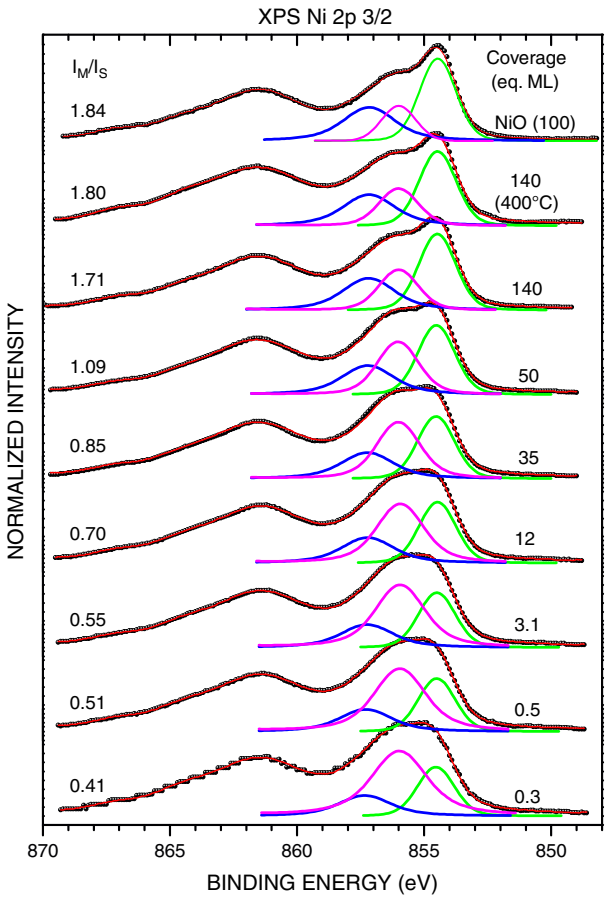

Fig. 4. Fittings of the Ni 2p 3/2 XPS spectra as a function of the equivalent coverage, in terms of the surface and nonlocal contributions as shown in Fig. 1. The spectrum of a NiO (100) single crystal is also shown for comparison. The corresponding intensity ratio of the main line to the surface peak (I_M/I_S) is also indicated.

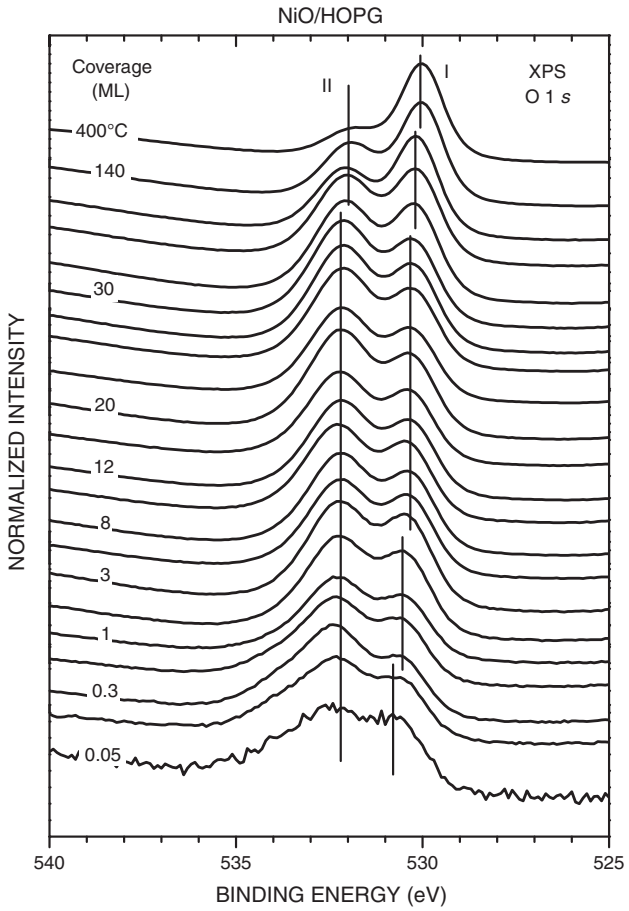

Fig. 5. O 1s XPS spectra of NiO deposited on HOPG as a function of the equivalent coverage.

after subtraction of the metallic Ni present in the core of the nanoparticles [21], exactly matches our spectra for intermediate coverages, indicating the nanometric size of the NiO nanostructures. The same happens in the analysis by Quases of NiO nanostructures presented by Ollivier et al. [23]. Other possible mechanisms to affect the shape of the Ni 2p XPS spectra such as strong modifications of the local crystalline structure and, possibly, stoichiometry in these nanospheres is ruled out according to the Ni 2p X-ray absorption spectra of the same stages of growth of the same experiment shown in Fig. 1 of ref. [14]. All the Ni 2p XAS spectra shown in this reference have the same high spin Ni^{2+} configuration with the same crystal field.

3.2. The O 1s XPS spectra

Fig. 5 shows the O 1s XPS spectra of NiO deposited on HOPG as a function of the coverage. These spectra present two different peaks located at about 530 eV and around 532 eV, although they shift slightly towards lower binding energies as the coverage increases. The spectra are dominated by the peak located at higher binding energies (532 eV) for coverage below 40 ML. On the other hand, the intensity of the peak at lower binding energies (530 eV) increases for larger coverage. The later becomes the most prominent in the spectrum of the annealed thin film. The peak at about 530 eV (O_I) comes from oxygen ions in the octahedral NiO_6 clusters in the NiO lattice, in agreement with other data reported in the literature for bulk NiO single crystal [26,27]. In contrast, the origin of the peak located at around 532 eV (O_{II}) is not clear, although it may also be related to surface effects.

Fig. 6 shows the I_M/I_S intensity ratio (solid circles), taken from the Ni 2p XPS spectra (see Fig. 2), as a function of the NiO coverage. It also presents the intensity ratio of the two oxygen peaks O_I/O_{II} (solid triangles), taken from the O 1s XPS spectra (see Fig. 5), as a function of the NiO coverage. Both ratios present very similar behavior, indicating that the formation of the oxygen species assigned to peak O_{II} can also be associated to surface effects. The oxygen ions located at the surface are affected by the lower effective hybridization with the Ni ions, due to the lack of an apical oxygen ion in the NiO_5

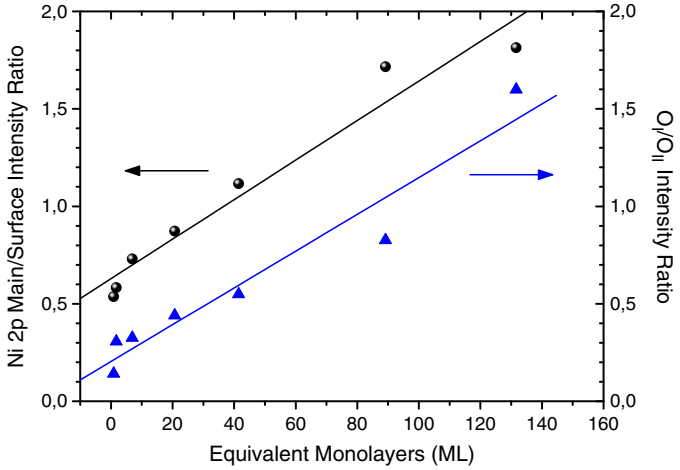

Fig. 6. Main line to surface peaks intensity ratio (I_M/I_S) of the Ni 2p XPS (solid circles), as well as O_I to O_{II} peaks intensity ratio (O_I/O_{II}) of the O 1s XPS (solid triangles), as a function of the equivalent coverage.

pyramid. This effect produces not only the shoulder in the Ni 2p XPS spectra, about 1.5 eV from the main line, but also the O_{II} peak in the O 1s XPS spectra, around 2 eV from the O_I peak.

Attempting a quantitative analysis in order to estimate the Ni/O ratio for the bulk and surface peaks with respect to the O_I and O_{II} peaks respectively is a very hard task. This is mainly due to the difficulty in the determination of the photoemission cross sections for the bulk and surface peaks separately of the Ni 2p XPS spectra. For instance, according to [25] the photoemission cross section for the Ni 2p spectra is 4.5 whereas for the Ni $2p_{3/2}$ is 3. Taking into account that the Ni $2p_{3/2}$ spectrum is dominated by the intensity of the charge transfer satellite at about 862 eV binding energy, the corresponding cross sections of the bulk and surface peaks should be significantly reduced from the above value. On the other hand these values should be equal since they account for the photoionization of orbitals of the same character. According to this, for a value of 0.39 of the photoemission cross section of both peaks we obtain values of 0.98 and 1.43 for the Ni/O ratio in Ni (bulk)/OII and Ni (surface)/OI peaks respectively. These obtained values are in relative agreement with the 1.0 and 1.2 values given for the NiO_6 (bulk) and NiO_5 (surface) clusters. In any case, the values obtained for the Ni (surface)/OI peak are always larger than those obtained for the Ni (bulk)/OII peak.

The experimental results show that both XPS spectra are dominated by the surface contribution at low coverage, which in turn, is related to the relatively high surface-to-volume ratio of the corresponding NiO nanostructures.

4. Conclusions

We have studied the electronic structure of NiO nanostructures grown on graphite by means of XPS. In particular, we have shown that, for low coverage, the shoulder in the Ni 2p spectra is mostly related to the surface contribution. These results are consistent with the AFM images, which show the formation of ~10 nm NiO nanoparticles, giving the system a very high surface-to-volume ratio. Finally, the O 1s XPS spectra also show a surface related structure which follows the same trend observed in the Ni 2p spectra. The same approach could be used to study the surface effects on the electronic structure of other NiO nanostructures.

Acknowledgments

We want to thank the support of the MICINN of Spain under contracts CONSOLIDER-INGENIO FUNCOAT Ref. CSD2008-0023 and NANOSELECT Ref CSD2007-00041 and projects ENE2010 21198-C04-04 and MAT2011-26534 and the Comunidad de Madrid under contract NANOBIOMAGNET, Ref. S2009/MAT-1726. This work was also supported by Conselho Nacional de Desenvolvimento Científico e Tecnológico (CNPq) and Coordenação de Aperfeiçoamento de Pessoal de Nível Superior (CAPES).

References

[1] L. Soriano, I. Preda, A. Gutiérrez, S. Palacín, M. Abbate, A. Vollmer, Phys. Rev. B 75 (2007) 233417.
[2] R.J.O. Mossanek, I. Preda, M. Abbate, J. Rubio-Zuazo, G.R. Castro, A. Vollmer, A. Gutiérrez, L. Soriano, Chem. Phys. Lett. 501 (2011) 437.
[3] A. Fujimori, F. Minami, S. Sugano, Phys. Rev. B 29 (1984) 5225.
[4] G.A. Sawatzky, J.W. Allen, Phys. Rev. Lett. 53 (1984) 2339.
[5] S. Hüfner, Solid State Commun. 52 (1984) 793.
[6] M.J. Tomellini, J. Electron Spectrosc. Relat. Phenom. 58 (1992) 75.
[7] A.F. Carley, S.D. Jackson, J.N. O'Shea, M.W. Roberts, Surf. Sci. 440 (1999) L868.
[8] M.A. van Veenendaal, G.A. Sawatzky, Phys. Rev. Lett. 70 (1993) 2459.
[9] St. Uhlenbrock, Chr. Scharfschwerdt, M. Neumann, G. Illing, H.-J. Freund, J. Phys. Condens. Matter 4 (1992) 7973.
[10] F. Parmigiani, in: G. Pacchioni, et al., (Eds.), Cluster Models for Surface and Bulk Phenomena, vol. 1, Plenum Press, New York, 1992, p. 475.
[11] L. Sangaletti, L.E. Depero, F. Parmigiani, Solid State Commun. 103 (1997) 421.
[12] M. Taguchi, M. Matsunami, Y. Ishida, R. Eguchi, A. Chainani, Y. Takata, M. Yabashi, K. Tamasaku, Y. Nishino, T. Ishikawa, Y. Senba, H. Ohashi, S. Shin, Phys. Rev. Lett. 100 (2008) 206401.
[13] L. Soriano, A. Gutiérrez, I. Preda, S. Palacín, J.M. Sanz, M. Abbate, J.F. Trigo, A. Vollmer, P.R. Bressler, Phys. Rev. B 74 (2006) 193402.
[14] I. Preda, M. Abbate, A. Gutiérrez, S. Palacín, A. Vollmer, L. Soriano, J. Electron Spectrosc. Relat. Phenom. 156–158 (2007) 111.
[15] L. Soriano, M. Abbate, J. Vogel, J.C. Fuggle, A. Fernández, A.R. González-Elipe, M. Sacchi, J.M. Sanz, Chem. Phys. Lett. 208 (1993) 460.
[16] I. Preda, L. Soriano, L. Alvarez, J. Méndez, F. Yubero, A. Gutiérrez, J.M. Sanz, Surf. Interface Anal. 42 (2010) 869.
[17] S. Tougaard, QUASES, Software package for quantitative XPS/AES of surface nanostructures by inelastic peak shape analysissee, www.QUASES.com.
[18] V. Biju, M. Abdul Khadar, J. Nanopart. Res. 4 (2002) 247.
[19] P. Marcus, C. Hinnen, Surf. Sci. 392 (1997) 134.
[20] Z. Bastl, J. Franc, P. Janda, H. Pelouchová, Z. Samec, Nanotechnology 17 (2006) 1492.
[21] S. D'Addato, V. Grillo, S. Altieri, R. Tondi, S. Valeri, S. Frabboni, J. Phys. Condens. Matter 23 (2011) 175003.
[22] S. Valeri, S. Benedetti, P. Luches, J. Phys. Condens. Matter 19 (2007) 225002.
[23] E. Ollivier, J.P. Langeron, Surf. Interface Anal. 41 (2009) 295.
[24] I. Horcas, R. Fernández, J.M. Gómez-Rodríguez, J. Colchero, J. Gómez-Herrero, A.M. Baró, Rev. Sci. Instrum. 78 (2007) 013705.
[25] M.P. Seah, in: D. Briggs, M.P. Seah (Eds.), 2nd edition, Practical Surface Analysis, vol. 1, John Wiley and Sons, Chichester, 1990.
[26] J.M. McKay, V.E. Henrich, Phys. Rev. B 32 (1985) 6764.
[27] G. Tyuliev, P. Stefanov, M. Atanasov, J. Electron Spectrosc. Relat. Phenom. 63 (1993) 267.